

# The $J$ -triplet Cooper pairing with magnetic dipolar interactions

Yi Li and Congjun Wu

*Department of Physics, University of California, San Diego, CA 92093*

Recently cold atomic Fermi gases with the large magnetic dipolar interaction have been laser cooled. Different from electric-dipoles which are classic vectors, atomic magnetic dipoles are quantum-mechanical matrix operators proportional to hyperfine-spin of atoms, thus provide a rich opportunity to investigate exotic many-body physics. Furthermore, unlike anisotropic electric dipolar gases, unpolarized magnetic dipolar systems are isotropic under simultaneous spin-orbit rotation. These features provide a robust mechanism for a novel pairing symmetry: orbital  $p$ -wave ( $L = 1$ ) spin triplet ( $S = 1$ ) pairing with total angular momentum of the Cooper pair  $J = 1$ . Such a pairing is markedly different from both the  $^3\text{He-B}$  phase in which  $J = 0$  and the  $^3\text{He-A}$  phase in which  $J$  is not conserved. It is also different from the  $p$ -wave pairing in the single component electric dipolar systems in which spin degree of freedom does not exist.

PACS numbers: 03.75.Ss, 74.20.Rp, 67.30.H-, 05.30

Ultracold atomic and molecular systems with electric and magnetic dipolar interactions have become a research focus of cold atom physics [1–6]. When dipole moments are aligned by external fields, dipolar interactions exhibit the  $d_{r^2-3z^2}$ -type anisotropy. The anisotropic Bose-Einstein condensations of dipolar bosons (e.g.  $^{52}\text{Cr}$ ) have been observed [7–10]. For the fermionic electric dipolar systems,  $^{40}\text{K}$ - $^{87}\text{Rb}$  has been cooled down to nearly quantum-degeneracy [3]. Effects of the anisotropic electric dipolar interaction on the fermion many-body physics have been extensively investigated. In the Fermi liquid theory, both the single particle properties and collective excitations exhibit the  $d_{r^2-3z^2}$  anisotropy [11–16]. In the single component Fermi systems, the leading order Cooper pairing instability is in the  $p$ -wave channel. The anisotropy of the electric dipolar interaction renders the instability in the  $p_z$ -channel, which is slightly hybridized with other odd partial wave channels [19–26]. For the two-component cases, the dipolar interaction leads to the anisotropic spin triplet pairing, and its orbital partial wave is again in the  $p_z$ -channel [27–30]. The triplet pairing competes with the singlet pairing in the hybridized  $s + d_{r^2-3z^2}$ -channel. The mixing between the singlet and triplet pairings has a relative phase  $\pm\frac{\pi}{2}$ , which leads to a novel time-reversal symmetry breaking Cooper pairing state [28].

An important recent progress is the laser cooling and trapping of magnetic dipolar fermions of  $^{161}\text{Dy}$  and  $^{163}\text{Dy}$  with large atomic magnetic moments ( $10\mu_B$ ) [1, 2]. There are important differences between magnetic and electric dipolar interactions. Electric dipole moments are essentially non-quantized classic vectors from the mixing between the  $s$  and  $p$ -levels of molecule states, which are induced by external electric fields [3, 4], thus electric dipoles are frozen. In the absence of external fields, even though at each instant time there is a dipole moment of the heteronuclear molecule, it averages to zero at a long time scale. In contrast, magnetic dipole moments of atoms are intrinsic, proportional to their hyper-fine spins up to a Lande factor. Unpolarized magnetic dipolar Fermi systems are available in which dipoles are defrozen

as non-commutative quantum mechanical operators, thus leading to a richer quantum spin physics of dipolar interactions. Furthermore, the magnetic dipolar interaction is actually isotropic in the unpolarized systems. It is invariant under simultaneous spin-orbit rotations but not separate spin or orbit rotations. This spin-orbit coupling is different from usual single particle one, but an interaction effect. It plays an important role in the Fermi liquid properties such as the unconventional magnetic states and ferro-nematic states predicted by Fregoso *et al* [17, 18].

It is natural to expect that magnetic dipolar interaction brings novel pairing symmetries not studied in condensed matter systems before. The systems of  $^{161}\text{Dy}$  and  $^{163}\text{Dy}$  are with a very large hyperfine spin of  $F = \frac{21}{2}$ , thus their Cooper pairing problem is expected to be very challenging. As a first step, we study the simplest case of spin- $\frac{1}{2}$ , and find that the magnetic dipolar interaction provide a novel and robust mechanism to the  $p$ -wave ( $L = 1$ ) spin triplet ( $S = 1$ ) Cooper pairing to first order in interaction strength, which comes from the attractive part of the magnetic dipolar interaction. In comparison, the  $p$ -wave triplet pairing in usual condensed matter systems, such as  $^3\text{He}$  [31–33], is due to the spin-fluctuations mechanism, which is at second order in interaction strength (see Ref. [34, 35] for reviews). Such a mechanism is based on strong ferromagnetic tendency from the repulsive part of the  $^3\text{He}$ - $^3\text{He}$  interactions. Furthermore, the  $p$ -wave triplet Cooper pairing symmetry patterns in magnetic dipolar systems are novel, which do not appear in  $^3\text{He}$ . The orbital and spin angular momenta of the Cooper pair are entangled into the total angular momentum  $J = 1$ . In contrast, in the  $^3\text{He-B}$  phase [32],  $L$  and  $S$  combine into  $J = 0$ , and in the  $^3\text{He-A}$  phase,  $L$  and  $S$  are decoupled and  $J$  is not well-defined [31, 33]. There are two competing pairing possibilities in this  $J = 1$  channel with different values of  $J_z$ : the helical polar state ( $J_z = 0$ ) maintaining time reversal (TR) symmetry, and the axial state ( $J_z = \pm 1$ ) breaking TR symmetry. The helical polar state has point nodes and gapless Dirac spectra, which is a time-reversal invariant

generalization of the  $^3\text{He-A}$  phase with entangled spin and orbital degrees of freedom. In addition to the usual phonon mode, its Goldstone modes contain the total angular momentum wave as entangled spin-orbital modes.

We begin with the magnetic dipolar interaction between spin- $\frac{1}{2}$  fermions

$$V_{\alpha\beta,\beta'\alpha'}(\vec{r}) = \frac{\mu^2}{r^3} \{ \vec{S}_{\alpha\alpha'} \cdot \vec{S}_{\beta\beta'} - 3(\vec{S}_{\alpha\alpha'} \cdot \hat{r})(\vec{S}_{\beta\beta'} \cdot \hat{r}) \}, \quad (1)$$

where  $\vec{r}$  is the relative displacement vector between two fermions;  $\mu$  is the magnitude of the magnetic moment. Such an interaction is invariant under the combined  $SU(2)$  spin rotation and  $SO(3)$  space rotation. In other words, orbital angular momentum  $\vec{L}$  and spin  $\vec{S}$  are not separately conserved, but the total angular momentum  $\vec{J} = \vec{L} + \vec{S}$  remains conserved. Its Fourier transform reads [18]

$$V_{\alpha\beta,\beta'\alpha'}(\vec{q}) = \frac{4\pi}{3} \mu^2 \{ 3(\vec{S}_{\alpha\alpha'} \cdot \hat{q})(\vec{S}_{\beta\beta'} \cdot \hat{q}) - \vec{S}_{\alpha\alpha'} \cdot \vec{S}_{\beta\beta'} \}. \quad (2)$$

The Hamiltonian in the second quantization form is written as

$$H = \sum_{\vec{k},\alpha} [\epsilon(\vec{k}) - \mu_c] c_{\alpha}^{\dagger}(\vec{k}) c_{\alpha}(\vec{k}) + \frac{1}{2V} \sum_{\vec{k},\vec{k}',\vec{q}} V_{\alpha\beta,\beta'\alpha'}(\vec{k} - \vec{k}') P_{\alpha\beta}^{\dagger}(\vec{k};\vec{q}) P_{\beta'\alpha'}(\vec{k}';\vec{q}), \quad (3)$$

where  $\epsilon(\vec{k}) = \hbar k^2/(2m)$ ;  $\mu_c$  is the chemical potential;  $P_{\beta'\alpha'}(\vec{k};\vec{q}) = c_{\beta'}(-\vec{k} + \vec{q}) c_{\alpha'}(\vec{k} + \vec{q})$  is the pairing operator; the Greek indices  $\alpha, \beta, \alpha'$  and  $\beta'$  refer to  $\uparrow$  and  $\downarrow$ ;  $V$  is the system volume. We define a dimensionless interaction strength parameter as the ratio between the characteristic interaction energy and the Fermi energy:  $\lambda \equiv E_{int}/E_F = \frac{2}{3} \frac{\mu^2 m k_f}{\pi^2 \hbar^2}$ .

Before analyzing the momentum space pairing, which is accurate in the weak-coupling limit. We first present a heuristic picture of the two-body pairing problem in the strong coupling limit without the Fermi surface. An important feature of the magnetic dipolar interaction (Eq. 1) is that it vanishes in the total spin singlet channel, thus we only need to study the triplet pairing in odd orbital partial wave channels. Dipolar interaction has a characteristic length scale  $a_{dp} = m\mu^2/\hbar^2$  at which the kinetic energy scale equals the interaction energy scale. We are not interested in solving the radial equation but focus on the symmetry properties of the angular solution, thus we fix the distance between two spins at  $a_{dp}$ . We will see later that partial wave channels  $L > 1$  have negligible contributions, and thus only consider the orbital  $p$ -wave channel here. The  $3 \times 3 = 9$  states ( $L = S = 1$ ) are classified into three sectors of  $J = 0, 1$  and 2. In each channel of  $J$ , the interaction energies are diagonalized as

$$E_0 = E_{dp}, \quad E_1 = -\frac{1}{2}E_{dp}, \quad E_2 = \frac{1}{10}E_{dp}, \quad (4)$$

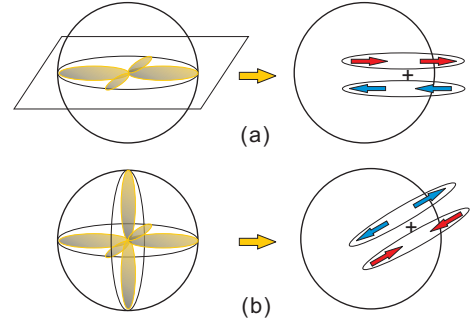


FIG. 1: The spin configurations of the two-body states with a)  $j=1$  and  $j_z = 0$  and b)  $j = j_z = 0$ . The interactions are attractive in a) but repulsive in b).

respectively, where  $E_{dp} = \mu^2/a_{dp}^3$ . Only the total angular momentum triplet sector with  $J = 1$  supports bound states, thus is the dominant pairing channel in the strong coupling limit.

This result can be understood intuitively from the spin configurations in the  $J$ -triplet sector. The fact that the attractive interaction exists in the  $J$ -triplet sector can be understood from their spin configurations. We define that  $\chi_{\mu}$  and  $p_{\mu}(\hat{\Omega})$  are eigenstates with the zero eigenvalue for operators  $\hat{e}_{\mu} \cdot (\vec{S}_1 + \vec{S}_2)$  and  $\hat{e}_{\mu} \cdot \vec{L}$  ( $\mu = x, y, z$ ), which are the total spin and orbital angular momenta projecting along the  $e_{\mu}$ -direction. The  $J$ -triplet sector states are  $\phi_{\mu}(\Omega) = \frac{1}{\sqrt{2}} \epsilon_{\mu\nu\lambda} \chi_{\nu} p_{\lambda}(\Omega)$  and  $\phi_{\mu}$  satisfies  $(\hat{e}_{\mu} \cdot \vec{J})\phi_{\mu} = 0$ . For example,

$$\begin{aligned} \phi_z(\hat{\Omega}) &= \frac{1}{\sqrt{2}} [\chi_x p_y(\hat{\Omega}) - \chi_y p_x(\hat{\Omega})] \\ &= \sqrt{\frac{3}{2}} \sin \theta \{ |\alpha_{\hat{e}_\rho}\rangle_1 |\alpha_{\hat{e}_\rho}\rangle_2 + |\beta_{\hat{e}_\rho}\rangle_1 |\beta_{\hat{e}_\rho}\rangle_2 \}, \end{aligned} \quad (5)$$

where  $\hat{e}_{\rho} = \hat{x} \cos \phi + \hat{y} \sin \phi$  and  $|\alpha_{\hat{e}_\rho}\rangle$  and  $|\beta_{\hat{e}_\rho}\rangle$  are eigenstates of  $\hat{e}_{\rho} \cdot \vec{\sigma}$  with eigenvalues of  $\pm 1$ . As depicted in Fig. 1 A, along the equator where  $\phi_z$  has the largest weight, two spins are parallel and along  $\hat{r}$ , thus the interaction is dominated by attraction. On the other hand, the eigenstate of  $J = 0$  reads

$$\phi_0(\Omega) = \chi_{\mu} p_{\mu}(\Omega) = \frac{1}{\sqrt{2}} \{ |\alpha_{\Omega}\rangle_1 |\beta_{\Omega}\rangle_2 + |\beta_{\Omega}\rangle_1 |\alpha_{\Omega}\rangle_2 \}, \quad (6)$$

where  $|\alpha_{\Omega}\rangle$  and  $|\beta_{\Omega}\rangle$  are eigenstates of  $\hat{\Omega} \cdot \vec{\sigma}$  with eigenvalues of  $\pm 1$ . As in Fig. 1 B, along any direction of  $\hat{\Omega}$ , two spins are anti-parallel and longitudinal, thus the interaction is repulsive.

We next prove that the same pairing symmetry pattern appears in the presence of Fermi surface, i.e., in the weak coupling theory. Considering the uniform pairing states at the mean-field level, we set  $\vec{q} = 0$  in Eq. 3, and define triplet pairing operators  $P_s(\vec{k})$  which are eigen-operators of  $\vec{S}_{1z} + \vec{S}_{2z}$  with eigenvalues  $s_z = 0, \pm 1$ , respectively. More explicitly, they are  $P_0(\vec{k}) = \frac{1}{\sqrt{2}} [P_{\uparrow\downarrow}(\vec{k}) + P_{\downarrow\uparrow}(\vec{k})]$ ,

$P_1(\vec{k}) = P_{\uparrow\uparrow}(\vec{k})$ ,  $P_{-1}(\vec{k}) = P_{\downarrow\downarrow}(\vec{k})$ . The pairing interaction of Eq. 3 reduces to

$$H_{pair} = \frac{1}{2V} \sum_{\vec{k}, \vec{k}', s_z s'_z} \left\{ V_{s_z s'_z}^T(\vec{k}; \vec{k}') P_{s_z}^\dagger(\vec{k}) P_{s'_z}(\vec{k}') \right\} \quad (7)$$

where

$$V_{s_z s'_z}^T(\vec{k}; \vec{k}') = \frac{1}{2} \sum_{\alpha\beta\beta'\alpha'} \langle 1s_z | \frac{1}{2} \alpha \frac{1}{2} \beta \rangle \langle 1s'_z | \frac{1}{2} \alpha' \frac{1}{2} \beta' \rangle^* \left\{ V_{\alpha\beta, \beta'\alpha'}(\vec{k} - \vec{k}') - V_{\alpha\beta, \beta'\alpha'}(\vec{k} + \vec{k}') \right\}, \quad (8)$$

where  $\langle 1s_z | \frac{1}{2} \alpha \frac{1}{2} \beta \rangle$  is the Clebsch-Gordan coefficient for two spin- $\frac{1}{2}$  states to form the spin triplet;  $V_{s_z s'_z}(\vec{k}; \vec{k}')$  is an odd function of both  $\vec{k}$  and  $\vec{k}'$ .

The decoupled mean-field Hamiltonian reads

$$H_{mf} = \frac{1}{2V} \sum_{\vec{k}} \Psi^\dagger(\vec{k}) \begin{pmatrix} \xi(\vec{k})I & \Delta_{\alpha\beta}(\vec{k}) \\ \Delta_{\beta\alpha}^*(\vec{k}) & -\xi(\vec{k})I \end{pmatrix} \Psi(\vec{k}), \quad (9)$$

where we only sum over half of the momentum space;  $\xi(\vec{k}) = \epsilon(\vec{k}) - \mu_c$ ;  $\Psi(\vec{k}) = (c_\uparrow(\vec{k}), c_\downarrow(\vec{k}), c_\uparrow(-\vec{k}), c_\downarrow(-\vec{k}))^T$ ;  $\Delta_{\alpha\beta}$  is defined as  $\Delta_{\alpha\beta} = \sum_{s_z} \langle 1s_z | \frac{1}{2} \alpha \frac{1}{2} \beta \rangle^* \Delta_{s_z}$ .  $\Delta_{s_z}$  satisfies the mean-field gap function as

$$\Delta_{s_z}(\vec{k}) = \frac{1}{V} \sum_{\vec{k}', s'_z} V_{s_z s'_z}^T(\vec{k}; \vec{k}') \langle P_{s'_z}(\vec{k}') | \rangle \\ = - \int \frac{d^3 k'}{(2\pi)^3} V_{s_z s'_z}^T(\vec{k}; \vec{k}') \left[ K(\vec{k}') - \frac{1}{2\epsilon_k} \right] \Delta_{s'_z}(\vec{k}'), \quad (10)$$

where  $K(\vec{k}') = \tanh[\frac{\beta}{2} E_i(\vec{k}')]/[2E_i(\vec{k}')]$ . The integral in Eq. 10 is already normalized following the standard procedure [19]. The Bogoliubov quasiparticle spectra become  $E_{1,2}(\vec{k}) = \sqrt{\xi_k^2 + \lambda_{1,2}^2(\vec{k})}$  where  $\lambda_{1,2}^2(\vec{k})$  are the eigenvalues of the positive-definite Hermitian matrix  $\Delta^\dagger(\vec{k})\Delta(\vec{k})$ . The free energy can be calculated as

$$F = -\frac{2}{\beta} \sum_{\vec{k}, i=1,2} \ln \left[ 2 \cosh \frac{\beta E_{\vec{k}, i}}{2} \right] - \frac{1}{2V} \\ \times \sum_{\vec{k}, \vec{k}', s_z, s'_z} \left\{ \Delta_{s_z}^*(\vec{k}) V_{s_z s'_z}^{T,-1}(\vec{k}; \vec{k}') \Delta_{s'_z}(\vec{k}') \right\}, \quad (11)$$

where  $V_{s_z s'_z}^{T,-1}(\vec{k}; \vec{k}')$  is the inverse of the interaction matrix defined as

$$\frac{1}{V} \sum_{\vec{k}', s'_z} V_{s_z s'_z}^T(\vec{k}; \vec{k}') V_{s'_z s'''}^{T,-1}(\vec{k}'; \vec{k}'') = \delta_{\vec{k}, \vec{k}'} \delta_{s_z, s''}. \quad (12)$$

We next linearize Eq. 10 around  $T_c$  and perform the partial wave analysis to determine the dominant pairing channel. Since the total angular momentum is conserved, we can use  $J$  to classify the eigen-gap functions denoted

as  $\phi_{s_z}^{a, JJ_z}(\vec{k})$ . The index  $a$  is used to distinguish different channels sharing the same value of  $J$ .  $\phi_{s_z}^{a, JJ_z}(\vec{k})$  satisfies

$$N_0 \int \frac{d\Omega_{k'}}{4\pi} V_{s_z s'_z}^T(\vec{k}; \vec{k}') \phi_{s'_z}^{a, JJ_z}(\vec{k}') = w_J^a \phi_{s_z}^{a, JJ_z}(\vec{k}), \quad (13)$$

where  $N_0 = \frac{mk_f}{\pi^2 \hbar^2}$  is the density of state at the Fermi surface;  $w_J^a$  are dimensionless eigenvalues;  $\vec{k}, \vec{k}'$  are at the Fermi surface. Then Eq. 10 is linearized into a set of decoupled equations

$$\phi^{a, JJ_z} \{ 1 + w_J^a [\ln(2e^\gamma \bar{\omega}) / (\pi k_B T)] \} = 0, \quad (14)$$

where  $\bar{\omega}$  is an energy scale at the order of Fermi energy playing the role of the momentum space cut off.

The spherical harmonics decomposition of  $V_{s_z s'_z}^T(\vec{k}; \vec{k}')$  can be formulated as

$$\frac{N_0}{4\pi} V_{s_z s'_z}(\vec{k}; \vec{k}') \\ = \sum_{Lm, L'm'} V_{Lm s_z; L'm' s'_z} Y_{Lm}^*(\Omega_k) Y_{L'm'}(\Omega_{\vec{k}'}), \quad (15)$$

where  $L = L'$  or  $L = L' \pm 2$ , and  $L, L'$  are odd numbers. The expressions of the dimensionless matrix elements  $V_{Lm s_z; L'm' s'_z}$  are very lengthy and will be presented elsewhere. After diagonalizing this matrix, we find the most negative eigenvalue is  $w^{J=1} = -3\pi\lambda/4$  lying in the channel with  $J = L = 1$ . All other negative eigenvalues are significantly smaller. Thus the dominant pairing channel remains in the  $J$ -triplet channel in the weak coupling theory.

We next study the competition between the three pairing branches in the  $J$ -triplet channel under the Ginzburg-Landau (GL) framework. We define  $\Delta_x(\vec{k}) = \frac{1}{\sqrt{2}} [-\Delta_1(\vec{k}) + \Delta_{-1}(\vec{k})]$ ,  $\Delta_y(\vec{k}) = \frac{i}{\sqrt{2}} [\Delta_1(\vec{k}) + \Delta_{-1}(\vec{k})]$ ,  $\Delta_z(\vec{k}) = \Delta_0(\vec{k})$ . The bulk pairing order parameters are defined as  $\Delta_\mu = \frac{1}{V} \sum_{\vec{k}} \hat{k}_\mu \Delta_\mu(\vec{k})$  where no summation over  $\mu$  is assumed. We define pairing parameters and their real and imaginary parts as the following 3-vectors  $\vec{\Delta} = (\Delta_x, \Delta_y, \Delta_z)$ . The GL free energy is constructed to maintain the  $U(1)$  and  $SO(3)$  rotational symmetry as

$$F = \alpha \vec{\Delta}^* \cdot \vec{\Delta} + \gamma_1 |\vec{\Delta}^* \cdot \vec{\Delta}|^2 + \gamma_2 |\vec{\Delta}^* \times \vec{\Delta}|^2, \quad (16)$$

where  $\alpha = N_0 \ln(\frac{T}{T_c})$  and  $T_c \approx \frac{2e^\gamma \bar{\omega}}{\pi} e^{-\frac{1}{|w^{J=1}|}}$ . The sign of  $\gamma_2$  determines two different pairing structures:  $\text{Re} \vec{\Delta} \parallel \text{Im} \vec{\Delta}$  at  $\gamma_2 > 0$ , and  $\text{Re} \vec{\Delta} \perp \text{Im} \vec{\Delta}$  at  $\gamma_2 < 0$ , respectively. Using the analogy of the spinor condensation of spin-1 bosons, the former is the polar pairing state and the latter is the axial pairing state [36–38].

For the polar pairing state, the order parameter configuration can be conveniently denoted as  $\vec{\Delta} = e^{i\phi} |\Delta| \hat{z}$  up to a  $U(1)$  phase and  $SO(3)$ -rotation. Such pairing carries the quantum number  $J_z = 0$ . The pairing matrix  $\Delta_{\alpha\beta}^{pl} = \frac{1}{2} |\Delta| [k_y \sigma_1 - k_x \sigma_2]_{\alpha\beta}$ , which reads

$$\Delta_{\alpha\beta}^{pl} = \frac{1}{2} |\Delta| \begin{bmatrix} -(\hat{k}_y + i\hat{k}_x) & 0 \\ 0 & \hat{k}_y - i\hat{k}_x \end{bmatrix}. \quad (17)$$

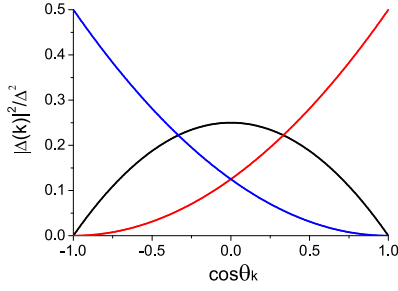


FIG. 2: The angular distribution of the gap function  $|\Delta(\vec{k})|^2$  v.s.  $\cos \theta_k$  in the helical polar pairing state (the red line) and the axial pairing state (the black lines).

It equivalents to a superposition of  $p_x \mp ip_y$  orbital configurations for spin- $\uparrow\uparrow$  ( $\downarrow\downarrow$ ) pairs, respectively, thus it is also helical. It is a unitary pairing state because  $\hat{\Delta}^\dagger \hat{\Delta}$  is proportional to a  $2 \times 2$  identity matrix. The Bogoliubov quasiparticle spectra are degenerate for two different spin configurations as  $E_{k,\alpha}^{pl} = \sqrt{\xi_k^2 + |\Delta^{pl}(\vec{k})|^2}$  with the anisotropic gap function  $|\Delta^{pl}(\vec{k})|^2 = \frac{1}{4}|\Delta|^2 \sin^2 \theta_k$  depicted in Fig. 2. They exhibit Dirac cones at north and south poles with opposite chiralities for two spin configurations.

Similarly, the order parameter configuration in the axial pairing state can be chosen as  $\vec{\Delta} = \frac{1}{\sqrt{2}}e^{i\phi}|\Delta|(\hat{e}_x + i\hat{e}_y)$  up to the symmetry transformation. This state carries the quantum number of  $J_z = 1$ . The pairing matrix  $\Delta_{\alpha\beta}^{ax} = \frac{1}{2\sqrt{2}}|\Delta|\{[\hat{k}_z(\sigma_1 + i\sigma_2) + \sigma_z(\hat{k}_x + i\hat{k}_y)]i\sigma_2\}_{\alpha\beta}$ , takes the form of

$$\Delta_{\alpha\beta}^{ax} = \frac{\sqrt{2}}{2}|\Delta| \begin{bmatrix} \hat{k}_z & \frac{1}{2}(\hat{k}_x + i\hat{k}_y) \\ \frac{1}{2}(\hat{k}_x - i\hat{k}_y) & 0 \end{bmatrix}. \quad (18)$$

This is a non-unitary pairing state since  $\Delta^\dagger \Delta = |\Delta|^2[\frac{1}{2}(1 + \hat{k}_z^2) + \hat{k}_z(\vec{k} \cdot \vec{\sigma})]$ . The Bogoliubov quasiparticle spectra have two non-degenerate branches with anisotropic dispersion relations as  $E_{1,2}^{ax}(\vec{k}) = \sqrt{\xi_k^2 + |\Delta_{\pm}^{ax}(\vec{k})|^2}$ . The angular gap distribution  $|\Delta_{\pm}^{ax}(\vec{k})|^2 = \frac{1}{8}|\Delta|^2(1 \pm \cos \theta_k)^2$  is depicted in Fig. 2. Each of branch 1 and 2 exhibits one node at north pole and south pole, respectively. Around the nodal region, the dispersion simplifies into  $E_{1,2}(\vec{k}) = \sqrt{v_f^2(k_z \mp k_f)^2 + \frac{1}{32}|\Delta|^2(k_{\parallel}/k_f)^4}$  which is quadratic respect the the transverse momentum  $k_{\parallel} = \sqrt{k_x^2 + k_y^2}$ .

At the mean-field level, the helical polar pairing state is more stable than the axial state. Actually this conclusion is not so obvious as in the case of  $^3\text{He-B}$  phase, in which the isotropic gap function is the most stable among all the possible gap functions [32]. Here the gap functions are anisotropic in both the polar and helical pairing phases. We need to compare them by calculating their free energies from Eq. 11. The second term contributes the same to both, thus the difference only comes

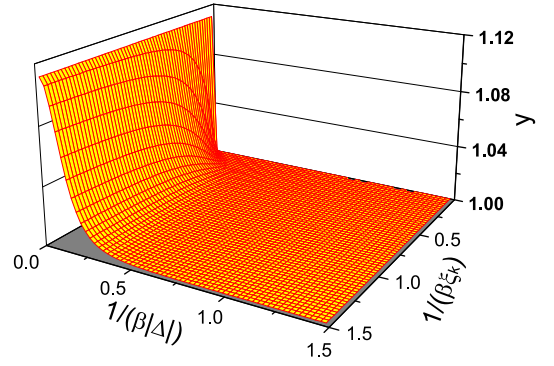


FIG. 3: The ratio of the angular integral of the free energy kernel  $y(\frac{1}{\beta|\Delta|}, \frac{1}{\beta|\xi_k|})$ , which is always larger than 1. This means that the polar pairing is favored at the mean-field level.

from the first term. We define the ratio of the angular integral of the free energy kernel in Eq. 11 as

$$y(\lambda_1, \lambda_2) = \frac{\int d\Omega_k 2 \ln \left[ 2 \cosh \frac{\beta}{2} \sqrt{\xi_k^2 + |\Delta^{pl}(\vec{k})|^2} \right]}{\int d\Omega_k \sum_{\pm} \ln \left[ 2 \cosh \frac{\beta}{2} \sqrt{\xi_k^2 + |\Delta_{\pm}^{ax}(\vec{k})|^2} \right]}, \quad (19)$$

where  $\lambda_1 = \frac{1}{\beta|\Delta|}$ ,  $\lambda_2 = \frac{1}{\beta|\xi_k|}$ .  $y(\lambda_1, \lambda_2)$  is numerically plotted in Fig. 3. For arbitrary values of  $\beta$ ,  $\xi_k$ , and  $|\Delta|$ ,  $y$  is always larger than 1, thus the polar state is favored than the axial state. This is because the convexity of the nonlinear term in Eq. 11, which favors isotropic angular distributions of  $|\Delta(\vec{k})|^2$  [39]. Although neither gap functions in these two states are absolutely isotropic as in the  $^3\text{He-B}$  phase, the polar gap function is more isotropic from Fig. 2 and thus is favored. However, we need to bear in mind that we cannot rule out the possibility that certain strong coupling effects can stabilize the axial state. In fact, the  $^3\text{He-A}$  phase can be stabilized under the spin feedback mechanism [34], which is a higher order effect in terms of interaction strength.

Next we discuss the classification of the Goldstone modes and vortices in these two states. In the helical polar state, the remaining symmetries are  $SO_J(2) \times Z_2$  as well as parity and time-reversal (TR), where  $Z_2$  means the combined operation of rotation  $\pi$  around any axis in the  $xy$ -plane and a flip of the pairing phase by  $\pi$ . The Goldstone manifold is

$$[SO_J(3) \times U_c(1)]/[SO_J(2) \otimes Z_2] = [S_J^2 \times U_c(1)]/Z_2. \quad (20)$$

The Goldstone modes include the phase phonon mode and two branches of spin-orbital modes. Vortices in this phase can be classified into the usual integer vortices in the phase sector and half-quantum vortices combined with  $\pi$ -disclination of the orientation of the  $\vec{\Delta}$ . In the axial state, the rotation around  $z$ -axis generates a shift of the pairing phase which can be canceled by a  $U_c(1)$  transformation, thus, the remaining symmetry is  $SO_{J_z-\phi}(2)$ . The Goldstone manifold is  $S^2 \times U_c(1)$ . Only integer vortices exist.

In summary, we have found that the magnetic dipolar interaction provide a robust mechanism at first order in interaction strength for a novel  $p$ -wave ( $L = 1$ ) spin triplet ( $S = 1$ ) Cooper pairing states, in which the total angular momentum of the Cooper pair is  $J = 1$ . This is a novel pairing pattern which does not appear in  $^3\text{He}$ , and to our knowledge, not in other condensed matter systems either. These states include the TR invariant helical polar pairing state and the TR breaking axial pairing state, both of which are distinct from the familiar  $^3\text{He-A}$  and  $B$  phases.

Many interesting questions are open for further explo-

ration including the topological properties of these pairing states, vortices and spin textures, and spectra of collective excitations. In the real experimental systems [1], the magnetic dipolar interaction is complicated by the large value of spin and the coupling between electron spin and orbital angular momenta inside atoms. The actual Cooper pairing structures in these systems will be investigated in a later publication.

C. W. thanks J. E. Hirsch for helpful discussions. Y. L and C. W. are supported by NSF under No. DMR-1105945, and Sloan Research Foundation.

- 
- [1] Lu, M., Youn, S. H. and Lev, B. L. Trapping ultracold dysprosium: a highly magnetic gas for dipolar physics. *Phys. Rev. Lett.* **104**, 63001 (2010).
- [2] Youn, S. H., Lu, M., Ray, U. and Lev, B. L. Dysprosium magneto-optical traps. *Phys. Rev. A* **82**, 043425 (2010).
- [3] Ospelkaus, S. *et al.* Ultracold polar molecules near quantum degeneracy. arXiv:0811.4618 (2008).
- [4] Ni, K. K. *et al.* A high phase-space-density gas of polar molecules. *Science* **322**, 231 (2008).
- [5] Griesmaier, A., Werner, J., Hensler, S., Stuhler, J. and Pfau, T. Bose-einstein condensation of chromium. *Phys. Rev. Lett.* **94**, 160401 (2005).
- [6] McClelland, J. J. and Hanssen, J. L. Laser cooling without repumping: a magneto-optical trap for erbium atoms. *Phys. Rev. Lett.* **96**, 143005 (2006).
- [7] Koch, T., Lahaye, T., Metz, J., Fröhlich, B., Griesmaier, A. and Pfau, T. Stabilization of a purely dipolar quantum gas against collapse. *Nat. Phys.* **4**, 218–222 (2008).
- [8] Lahaye, T., Menotti, C., Santos, L., Lewenstein, M. and Pfau, T. The physics of dipolar bosonic quantum gases. *Rep. Prog. Phys.* **72**, 126401 (2009).
- [9] Lahaye, T., Metz, J., Koch, T., Fröhlich, B., Griesmaier, A. and Pfau, T. A purely dipolar quantum gas. *21st International Conference on Atomic Physics*, 160. World Scientific, (2009).
- [10] Menotti, C., Lewenstein, M., Lahaye, T. and Pfau, T. Dipolar interaction in ultra-cold atomic gases. *Dynamics and Thermodynamics of Systems with Long Range Interactions: Theory and Experiments*, vol. 970, 332–361, (2008).
- [11] Sogo, T., He, L., Miyakawa, T., Yi, S., Lu, H. and Pu, H. Dynamical properties of dipolar fermi gases. *New J. Phys.* **11**, 055017 (2009).
- [12] Miyakawa, T., Sogo, T. and Pu, H. Phase-space deformation of a trapped dipolar fermi gas. *Phys. Rev. A* **77**, 061603 (2008).
- [13] Ronen, S. and Bohn, J. L. Zero sound in dipolar fermi gases. *Phys. Rev. A* **81**, 033601 (2010).
- [14] Chan, C. K., Wu, C., Lee, W. C. and Sarma, S. D. Anisotropic-fermi-liquid theory of ultracold fermionic polar molecules: Landau parameters and collective modes. *Phys. Rev. A* **81**, 023602 (2010).
- [15] Fregoso, B. M., Sun, K., Fradkin, E. and Lev, B. L. Biaxial nematic phases in ultracold dipolar fermi gases. *New J. Phys.* **11**, 103003 (2009).
- [16] Lin, C., Zhao, E. and Liu, W. V. Liquid crystal phases of ultracold dipolar fermions on a lattice. *Phys. Rev. B* **81**, 045115 (2010).
- [17] Fregoso, B. M. and Fradkin, E. Unconventional magnetism in imbalanced fermi systems with magnetic dipolar interactions. *Phys. Rev. B* **81**, 214443 (2010).
- [18] Fregoso, B. M. and Fradkin, E. Ferronematic ground state of the dilute dipolar fermi gas. *Phys. Rev. Lett.* **103**, 205301 (2009).
- [19] Baranov, M. A., Mar’enko, M. S., Rychkov, V. S., and Shlyapnikov, G. V. Superfluid pairing in a polarized dipolar fermi gas. *Phys. Rev. A* **66**, 013606 (2002).
- [20] Baranov, M. A., Dobrek, L. and Lewenstein, M. Superfluidity of trapped dipolar fermi gases. *Phys. Rev. Lett.* **92**, 250403 (2004).
- [21] Baranov, M. A. Theoretical progress in many-body physics with ultracold dipolar gases. *Physics Reports* **464**, 71–111 (2008).
- [22] You, L. and Marinescu, M. Prospects for p-wave paired bardeen-cooper-schrieffer states of fermionic atoms. *Phys. Rev. A* **60**, 2324 (1999).
- [23] Bruun, G. M. and Taylor, E. Quantum phases of a two-dimensional dipolar fermi gas. *Phys. Rev. Lett.* **101**, 245301 (2008).
- [24] Levinsen, J., Cooper, N. R. and Shlyapnikov, G. V. Topological  $p_x + ip_y$  superfluid phase of fermionic polar molecules. *Phys. Rev. A* **84**, 013603 (2011).
- [25] Potter, A. C., Berg, E., Wang, D. W., Halperin, B. I. and Demler, E. Superfluidity and Dimerization in a Multilayered System of Fermionic Polar Molecules. *Phys. Rev. Lett.* **105**, 220406 (2010).
- [26] Lutchyn, R. M., Rossi, E. and Das Sarma, S. Spontaneous interlayer superfluidity in bilayer systems of cold polar molecules. *Phys. Rev. A* **82**, 061604 (2010).
- [27] Samokhin, K. V. and Mar’enko, M. S. Nonuniform mixed-parity superfluid state in fermi gases. *Phys. Rev. Lett.* **97**, 197003 (2006).
- [28] Wu, C. and Hirsch, J. E. Mixed triplet and singlet pairing in ultracold multicomponent fermion systems with dipolar interactions. *Phys. Rev. B* **81**, 020508 (2010).
- [29] Shi, T., Zhang, J. N., Sun, C. P. and Yi, S. Singlet and triplet bcs pairs in a gas of two-species fermionic polar molecules. arXiv: 0910.4051 (2009).
- [30] Kain, B. and Ling, H. Y. Singlet and triplet superfluid competition in a mixture of two-component fermi and one-component dipolar bose gases. *Phys. Rev. A* **83**, 061603 (2011).

- [31] Anderson, P. W. and Morel, P. Generalized bardeen-cooper-schrieffer states and the proposed low-temperature phase of liquid  $\text{He}^3$ . *Phys. Rev.* **123**, 1911 (1961).
- [32] Balian, R. and Werthamer, N. R. Superconductivity with pairs in a relative p wave. *Phys. Rev.* **131**, 1553 (1963).
- [33] Brinkman, W. F., Serene, J. W. and Anderson, P. W. Spin-fluctuation stabilization of anisotropic superfluid states. *Phys. Rev. A* **10**, 2386 (1974).
- [34] Leggett, T. A theoretical description of the new phases of liquid  $^3\text{He}$ . *Rev. Mod. Phys.* **47**, 331 (1975).
- [35] Volovik, G.E. *The Universe in a Helium droplet.* Oxford University Press(2009).
- [36] Ho, T. L. Spinor bose condensates in optical traps. *Phys. Rev. Lett.* **81**, 742–745 (1998).
- [37] Zhou, F. Quantum spin nematic states in bose einstein condensates. *Int. J. Mod. Phys. B* **17**, 2643–2698 (2003).
- [38] Demler, E. and Zhou, F. Spinor bosonic atoms in optical lattices: symmetry breaking and fractionalization. *Phys. Rev. Lett.* **88**, 163001 (2002).
- [39] Cheng, M., Sun, K., Galitski, V. and Das Sarma, S. Stable topological superconductivity in a family of two-dimensional fermion models. *Phys. Rev. B* **81**, 024504 (2010).